Applied Thermal Engineering 129 (2018) 782–791

Contents lists available at ScienceDirect

Applied Thermal Engineering

journal homepage: www.elsevier.com/locate/apthermeng

Energy optimization for single mixed refrigerant natural gas liquefaction process using the metaheuristic vortex search algorithm

Wahid Ali [1], Muhammad Abdul Qyyum [1], Kinza Qadeer, Moonyong Lee *

School of Chemical Engineering, Yeungnam University, Gyeongsan 712-749, Republic of Korea

HIGHLIGHTS

- A modified refrigerants SMR process was optimized for NG liquefaction.
- Recently developed metaheuristic VSO algorithm was proposed.
- VSO generates the optimal results for the complex process outstandingly.
- Up to 41.5% energy was saved with COP of 32.8%.

GRAPHICAL ABSTRACT

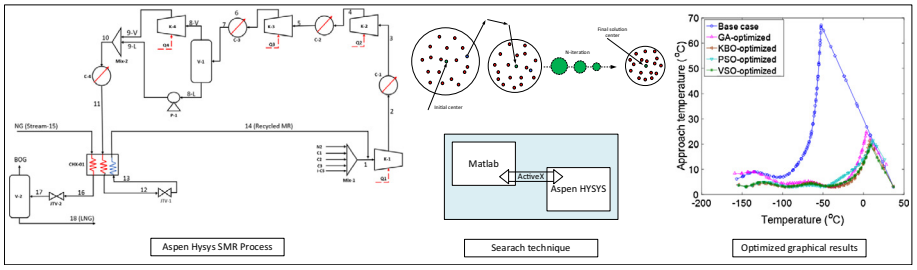

ARTICLE INFO

Article history:
Received 10 July 2017
Revised 15 September 2017
Accepted 12 October 2017
Available online 18 October 2017

Keywords:
LNG
Natural gas liquefaction
Single mixed refrigerant process
Metaheuristics
Vortex search optimization
Energy efficiency

ABSTRACT

A metaheuristic vortex search algorithm was investigated for the optimization of a single mixed refrigerant (SMR) natural gas liquefaction process. The optimal design of a natural gas liquefaction processes involves multivariable non-linear thermodynamic interactions, which lead to exergy destruction and contribute to process irreversibility. As key decision variables, the optimal values of mixed refrigerant flow rates and process operating pressures were determined in the vortex pattern corresponding to the minimum required energy. In addition, the rigorous SMR process was simulated using Aspen Hysys® software and the resulting model was connected with the vortex search optimization algorithm coded in MATLAB. The optimal operating conditions found by the vortex search algorithm significantly reduced the required energy of the single mixed refrigerant process by ≤41.5% and improved the coefficient of performance by ≤32.8% in comparison with the base case. The vortex search algorithm was also compared with other well-proven optimization algorithms, such as genetic and particle swarm optimization algorithms, and was found to exhibit a superior performance over these existing approaches.

1. Introduction

Despite the recent fall in oil and gas prices, the liquefied natural gas (LNG) industry remains active, with several new plants being planned for stationing through 2017 and 2018. Indeed, it is expected that by 2020, the LNG trade growth rate will increase by 50% [1], as the global energy demand is projected to grow by 48% between 2012 and 2040 [2]. Thus, to meet the worldwide LNG demand, continuous growth of the LNG industry is necessary over the coming decades. However, LNG production is generally considered to be a cost and energy intensive process, with the liquefaction facilities normally accounting for 40–50% [3] of the total LNG value chain cost and 1188 kJ/kg [4] energy is required to liquefy one kilogram natural gas. Although the cost and required energy for the natural gas liquefaction depends on the site conditions and the type of available liquefaction technologies.

To date, several LNG processes, such as dual mixed refrigerant (DMR), propane precooled mixed refrigerant (C3MR), and single mixed refrigerant (SMR) cycles for NG liquefaction have been widely employed for the base-load production of LNG. These

* Corresponding author.
E-mail address: mynlee@yu.ac.kr (M. Lee).
[1] These two authors contributed equally to this work.

https://doi.org/10.1016/j.applthermaleng.2017.10.078
1359-4311/

Nomenclature

N2	nitrogen
C1	methane
C2	ethane
C3	propane
iC5	iso-pentane
MITA	minimum internal temperature approach
C3MR	propane precooled mixed refrigerant
DMR	dual mixed refrigerant
KBO	knowledge-based optimization
NLP	non-linear programming
GA	genetic algorithm
PSO	particle swarm optimization
VSO	vortex search optimization
LNG	liquefied natural gas
MR	mixed refrigerant
NG	natural gas
SMR	single mixed refrigerant
TDCC	temperature difference between composite curves
THCC	temperature-heat flow between composite curves
LMTD	log mean temperature difference
COP	coefficient of performance

processes differ from one other in terms of capacity, degree of complexity, and performance. Among these processes, the SMR process (also known as PRICO® SMR technology) has been considered a suitable candidate for small-scale and offshore applications, due to its simple design, compactness, ease of operation, and small footprint [5–7].

The SMR process requires a significant energy input for its operation, with the main contribution to the energy requirement being the shaft work during the compression stage of the liquefaction cycle. This shaft work mainly depends on the temperature differences in the heat exchangers [8], with the temperature gradients in the main cryogenic heat exchanger being a function of operating pressures and mixed refrigerant flow rates. Rigorous optimization of the refrigerant flow rates and operating pressures can thereby improve the energy efficiency of SMR processes by reducing the gap between composite curves inside the LNG cryogenic exchanger [5,9], which will ultimately increase the global process competitiveness and lead to high economic benefits in terms of low energy intake. Indeed, the mixed refrigerant (MR) system for NG liquefaction was initially optimized by Ait-Ali [10], who employed a two-dimensional numerical search to determine the optimal solution. Later, Barnés and King [11] performed optimization of the pure refrigerant-based cascade process to minimize the total energy cost. To determine the optimal design for the MR-based LNG process, Lee et al. [12] established the optimal solution for the SMR process in terms of the minimum compression power. For this purpose, they employed non-linear programming (NLP) and thermodynamic approaches through manual observation of the composite curves. Shi et al. [13] employed thermodynamic simulation optimizer to reduce the unit power consumption for two-stage SMR, N_2-CH_4 expansion, and C3MR processes. In their work, a thermodynamic simulation sequential modular was used to simulate the LNG processes.

In recent years, process optimization has become more advanced and rigorous through the evolution of process modeling software, such as Aspen Hysys®, Pro-II®, and Honeywell Unisim™, which have extensive thermodynamic libraries. Indeed, the SMR process has been modeled and optimized using Aspen Hysys®, Aspen Plus®, Pro-II®, and Unisim™ through advanced optimization techniques, by developing connections between available optimization software (such as MATLAB, Microsoft Visual Studio (MVS), Microsoft Visual Basic (VBA), and GAMS) and simulators. For example, Mokarizadeh et al. [14] coded an objective function for the required compression power of the SMR process using MATLAB followed by optimization of the process using genetic algorithms (GA). In addition, Aspelund et al. [15] used a simulation-optimization framework for the optimal design of the SMR process. Nogal et al. [16] modeled the SMR process using Aspen Hysys® and then employed the GA and NLP for the design optimization of SMR process. Khan et al. [17] used nonlinear programming by linking MATLAB with the Unisim™ SMR model through the ActiveXcom server to increase the energy performance of the SMR process. Khan and Lee [5] minimized the energy efficiency of the SMR process by coding the particle swarm algorithm with non-linear constraints in the MATLAB environment and by linking it with the Honeywell Unisim Design™ SMR model. Shirazi and Mowla [14] used GA to minimize the required compression power for the SMR process. Morin et al. [18] proposed the evolutionary search algorithm for the design optimization of the SMR process. Tak et al. [19] simulated the SMR process using Aspen Hysys® and then used NLP to reduce the energy requirement for the LNG production. Cao et al. [20] proposed the robustness to adjust the mixed refrigerants composition in the SMR process corresponding to minimum required power. They optimized the SMR process using GA. Ding et al. [21] also used GA for the optimization of mixed refrigerant N_2-CH_4 based expansion liquefaction processes. Moreover, Park et al. [22] investigated the performance of the SMR process upon variation in the ambient air temperature, while optimizing the process using the particle swarm optimization (PSO) algorithm. Recently, Qyyum et al. [23] used the modified coordinate descent (MCD) approach to optimize the SMR process and presented the feasibility study of environmental relative humidity through the thermodynamic effects on the performance of the SMR process. Pham et al. [24] used the Coggins algorithm to optimize the modified SMR process, which was modeled in Aspen Hysys®. More specifically, they coded the Coggins algorithm in the MVS environment and then connected it with the Hysys model using the COM functionality.

It is therefore apparent that many existing optimization strategies adopt simplified models for feasible optimization, thereby compromising rigorous optimal results. In addition, the local minima and model convergence under infeasible key decision variables remain major issues associated with the NLP, GA, and PSO approaches. To solve these issues, Khan et al. [9] proposed a knowledge-based optimization (KBO) approach to determine the optimal values of the MR flow rates for the SMR and C3MR processes. In addition, Pham et al. [25] recently enhanced the SMR process to improve the energy efficiency through the addition of heavy hydrocarbons, such as *iso*-butane and *iso*-pentane to the conventional mixed refrigerant. They also employed the KBO technique for process optimization. However, the importance and benefits of the numerical optimization algorithms could not be ignored, with proficiency in terms of time-saving and complex problem solving being the major advantages of such algorithms.

Despite the significant research effort made in the development of an efficient optimization approach, the complex thermodynamics and highly non-linear interactions between the design variables involved in optimization of the SMR process render such optimization a challenging task. As such, a single-solution-based metaheuristic type optimization algorithm rather than a population-based or traditional stochastic algorithm is required

to optimize the SMR process in terms of lowering the compression power, which will ultimately increase the competitiveness of the process for both offshore and onshore LNG production. In this context, vortex-search optimization (VSO) has recently been introduced by Doğan and Ölmez [26], which is a single-solution metaheuristic algorithm. The main feature of the VSO is the adaptive step size scheme, which considerably enhances the performance of the search process, unlike the random search and pattern search algorithms. In addition, the search behavior of the VSO algorithm program is exhorted by the vortex pattern of stirred fluids. It uses a balance of explorative and exploitative behavior to determine the optimal objective. Therefore, at the beginning of the search, the algorithm acts in an explorative manner, resulting in an increase of the global search power. As the algorithm converges to a near optimal solution, it behaves in an exploitative mode to tune the present solution towards the optimum solution, and so the search radius decreases upon each iteration performed.

To analyze the efficiency of the VSO algorithm, the author employed this algorithm for the analog active filter component selection problem [27], and compared the results with other well-known algorithms, such as artificial bee colony (ABC), PSO2011, harmony search (HS), and differential evolution (DE), and concluded that VSO optimization was particularly effective. In addition, to measure the performance of the proposed optimization algorithm, Doğan and Yüksel [28] employed VSO for optimization of the analog filter group delay. In this case, the VSO exhaustively searched for a solution within the boundaries specified by the user, and converged towards a global solution for the problem [26–28]. The VSO algorithm is also advantageous in that it is a parameter-free algorithm unlike PSO2011 and ABS, among others [26].

Thus, we herein report investigation of the VSO algorithm for the bound-constrained optimal design solution of the non-linear SMR liquefaction process. The SMR process will be modeled using the Aspen Hysys® v.9 commercial simulator prior to linking the simulation model with the coded VSO algorithm using MATLAB. To validate the performance of the proposed algorithm, the results will also be compared with well-known algorithms such as GA, KBO, and PSO.

2. SMR process description and simulation

Fig. 1 shows a schematic representation of the enhanced SMR process. In this process, MR stream-1 containing a mixture of nitrogen, methane, ethane, propane, and *iso*-pentane, is utilized to liquefy the NG at approximately −159 °C and at a pressure slightly higher than atmospheric pressure. The MR is then compressed through a four-stage compression unit equipped with after-coolers/inter-stage coolers. After each compression stage, the heat is rejected from the MR through air-cooled coolers. The outlet temperature of inter-stage cooler was set at 40 °C except the inter-stage cooler C-2 (T_5) where the outlet temperature was set at 54.20 °C same as the base case [25] (see Table 3) to be above the dew point of stream-5. Finally, compressed MR is then introduced into the main cryogenic heat exchanger where it is fully condensed. Subsequently, the high-pressure liquid MR expands through a Joule-Thomson (JT) valve, and this expanded low temperature (approx. −155 °C) MR is evaporated by taking the latent heat of vaporization from the NG (stream-15) and the MR (stream-11). Finally, the superheated MR stream (stream-14) originating from the cryogenic heat exchanger is fed into the compressor (K-1) for recycling.

The SMR process reported in the previous study [25] was selected as the base example, and Aspen Hysys® v.9 was employed to simulate the SMR process. The NG feed conditions and the assumptions for the simulation are listed in Table 1. In addition, the Peng-Robinson model was employed to predict the binary interactions, while the Lee-Kesler equation was used to evaluate the entropies and enthalpies. A minimum internal temperature approach (MITA) of 3 °C [25,29] was selected to design the LNG cryogenic exchangers employed herein, and it was assumed that heat loss to the environment was negligible.

3. SMR process optimization

3.1. Objective function, constraints, and decision variables

Mixed refrigerant-based LNG processes are considered nonlinear issues in terms of optimization due to the number of extremely interactive relationships between the key decision variables and the constrained objective. Thus, even small changes in the decision variables can result in an unfeasible process. In this context, Table 2 lists the key decision variables of the SMR process along with their upper and lower bounds.

In this study, as in many recent studies [5,6,21,23,25,30], the energy efficiency in terms of specific compression power was selected as the objective function for optimization, and so the optimization problem could be formulated as follows:

$$\text{Min } f(X) = \text{Min.}\left(\sum_{i=1}^{n} W_i \Big/ m_{LNG}\right) \tag{1}$$

Subject to:

$$\Delta T_{(min)}(X) \geqslant 3 \tag{2}$$

where X is the decision variable vector, i.e., $X = (P_{10}, P_{13}, m_{N2}, m_{C1}, m_{C2}, m_{C3}, m_{iC5})$.

The flow rate of the refrigerant components, the condensation pressure, and the evaporation pressure were selected as the key decision variables, while a MITA value of 3 °C in the main cryogenic LNG exchanger and a zero liquid fraction at the inlet of each compressor were chosen as the constraints during optimization. All the constraints were then augmented into the objected function in the form of Lagrange penalty function.

3.2. VSO methodology

3.2.1. Initial guess solution

The working mechanism of the VSO algorithm can be explained using a vortex pattern. Fig. 2 shows a model of the VSO in a two-dimensional nested circle form. The outermost portion of the circle is taken as the first center of the search space (SS) within the bound, and the initial center (μ_0) of the SS can be calculated using Eq. (3), which represents the mean value of the upper and lower limits:

$$\mu_o = \frac{upper\_\text{lim} + lower\_lim}{2} \tag{3}$$

where the upper and lower limits are $d \times 1$ vectors that define the bound constraints of the problem in the dimensional space, d.

3.2.2. Candidate solutions

The neighbor solutions $C_i(X) = \{x_1, x_2, x_3, \ldots, x_k\}, k = 1, 2, \ldots, n$ (where n and i represent the total number of candidate solutions and the number of iterations, respectively) are randomly generated around the center using multivariate Gaussian methodology, as indicated in Eq. (4):

$$p(\zeta|\mu, \upsilon) = \frac{1}{\sqrt{(2\pi)^d|\upsilon|}} \exp\left(-\frac{1}{2}\frac{(\zeta-\mu)^T(\zeta-\mu)}{\upsilon}\right) \tag{4}$$

where d represents the dimension, ζ is the $d \times 1$ vector for a randomly generated variable, μ is the $d \times 1$ vector of the sample mean (taken as the center), and v is the covariance matrix. The value of v

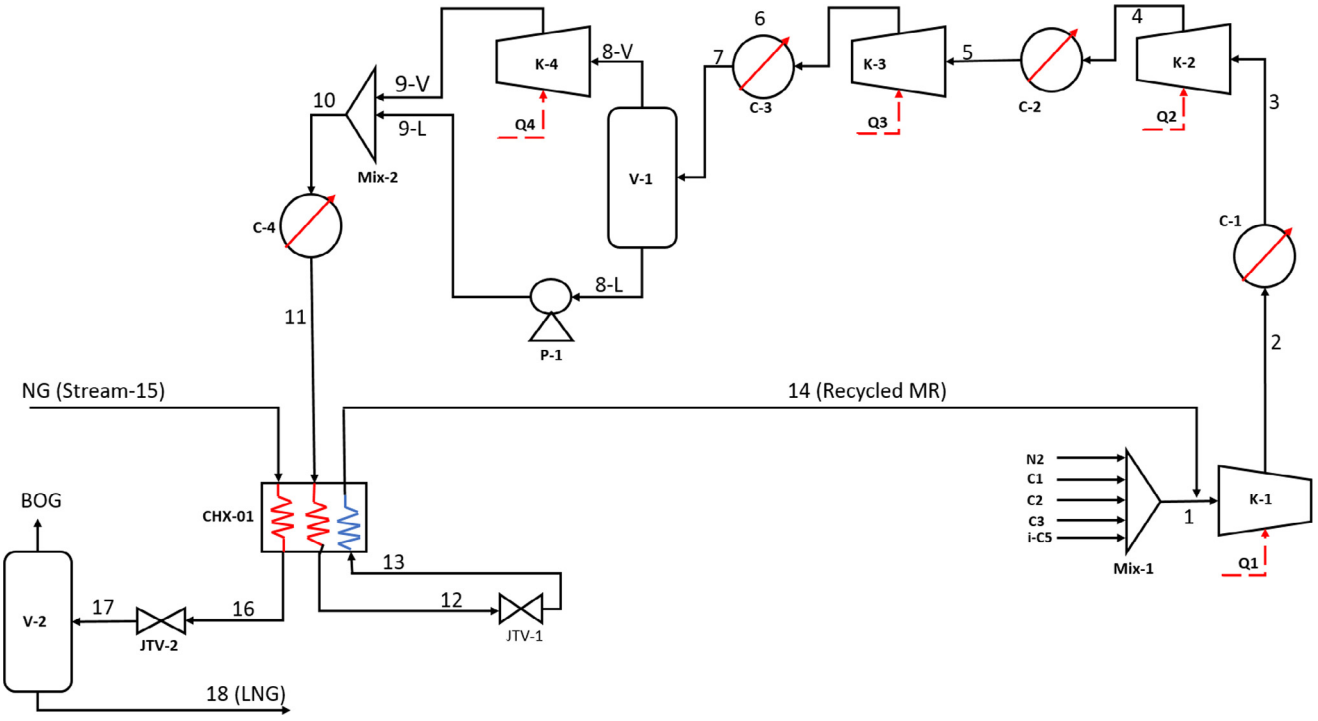

Fig. 1. Process flow diagram for the SMR process.

Table 1
NG feed conditions and assumptions for simulation of the SMR process [25]

Property	Condition
NG feed condition	
Temperature	32 °C
Pressure	80 bar
Flow rate	1.0 kg/h
NG feed composition	*Mole fraction*
Nitrogen	0.0022
Methane	0.9133
Ethane	0.0536
Propane	0.0214
i-Butane	0.0046
n-Butane	0.0047
i-Pentane	0.001
n-Pentane	0.001
Intercooler outlet temperature	40 °C
Vapor fraction boil-off-gas	8.0%
Compressor isentropic efficiency	0.75
Pump isentropic efficiency	0.75
Thermodynamic property package	Peng-Robinson
Enthalpy calculation	Lee Kesler
Pressure drops across LNG heat exchanger	
"Stream-15" to "Stream-16"	1.0 bar (hot stream)
"Stream-11" to "Stream-12"	1.0 bar (hot stream)
"Stream-13" to "Stream-14"	0.1 bar (cold stream)

Table 2
Key decision variables of the SMR process and their upper and lower bounds.

Decision variables	Lower bound	Upper bound
High pressure of MR, P_{10} (bar)	35.0	70.0
Evaporation pressure, P_{13} (bar)	1.1	4.0
Flow rate of nitrogen, m_{N2} (kg/h)	0.1	0.75
Flow rate of methane, m_{C1} (kg/h)	0.15	0.85
Flow rate of ethane, m_{C2} (kg/h)	0.45	1.15
Flow rate of propane, m_{C2} (kg/h)	0.55	1.40
Flow rate of *iso*-pentane, m_{iC5} (kg/h)	0.65	1.85

can be computed using Eq. (5). Additional detailed information can be found in the literature [26].

$$\upsilon = s^2 \cdot [I]_{d\times d} \tag{5}$$

where s^2 represents the variance of the distribution, and I represents the $d \times d$ identity matrix. The initial standard deviation (s_0) can then be calculated using Eq. (6):

$$s_o(=r_o) = \frac{\max(upper\_\lim) - \min(lower\_\lim)}{2} \tag{6}$$

where s_0 can also be taken as the initial radius (r_0), which is initially selected as a large value to achieve full coverage of the SS (weak locality).

3.2.3. Substitution of the current solution

In the selection phase, the best solution $X' \in C_o(X)$, $(i = 0)$ is selected and memorized from $C_0(X)$ to replace the current circle center μ_0. Prior to the choice phase, the candidate solutions must be within the search boundaries, as shown in Eq. (7):

$$lower\_\lim^d \leqslant s_k^d \leqslant upper\_\lim^d \tag{7}$$

where $k = 1, 2, \ldots, n$, and d represents the dimensions. In the subsequent iteration, the learned best solution X' is attributed to the center of the next circle, while in the second step of the generation phase, the effective radius (r_1) of this circle is reduced, and a new set of solutions $C_1(X)$ is obtained around the new center. It should be noted that in the second step, the locality of the obtained neighbor solutions increases with the decreased radius. In the selection phase of the second step, the new set of solutions $C_1(X)$ is evaluated to select a solution where $X' \in C_1(X)$.

If the chosen solution is superior to the previous solutions, then this solution is appointed as the new best solution and it is saved. In the subsequent phase, the appointed center of the third phase is memorized as the best solution up to that point, and this process continues until the minimum function evaluation termination criterion is reached. Fig. 2 provides an exemplifying study of the

Table 3
Summary and comparison of the optimization results of the VSO methodology with other well-known optimization algorithms.

	Base case [25]	KBO Optimized [25]	GA optimized	PSO optimized	VSO optimized
Decision variables					
High pressure of MR, P_{10} (bar)	46.1	48.75	55.0	59.0	52.0
Evaporation Pressure of MR, P_{13} (bar)	1.3	2.22	2.6	3.4	3.8
Flow rate of nitrogen, m_{N2} (kg/h)	0.2690	0.2660	0.1956	0.2981	0.3295
Flow rate of methane, m_{C1} (kg/h)	0.5290	0.4850	0.5848	0.5412	0.5100
Flow rate of ethane, m_{C2} (kg/h)	0.6190	0.7950	0.5714	0.7200	0.9500
Flow rate of propane, m_{C2} (kg/h)	2.847	0.7100	1.1500	1.1200	0.6890
Flow rate of *iso*-pentane, m_{iC5} (kg/h)	0.0	1.5000	1.1000	1.2500	1.415
Constraints					
MITA (°C)	3.0	3.0	3.0	3.0	3.0
T_3 (°C)	40.0	40.0	40.0	40.0	40.0
T_5 (°C)	40.0	54.20	46.0	53.0	54.20
T_{14} (°C)	36.93	36.80	36.92	24.69	36.96
Specific compression power (kW/kg-LNG)	**0.4584**	**0.3183**	**0.2887**	**0.2808**	**0.2681**
Relative energy saving (%)	–	**30.6**	**37.0**	**38.7**	**41.5**

These values are bold to emphasize the main research findings.

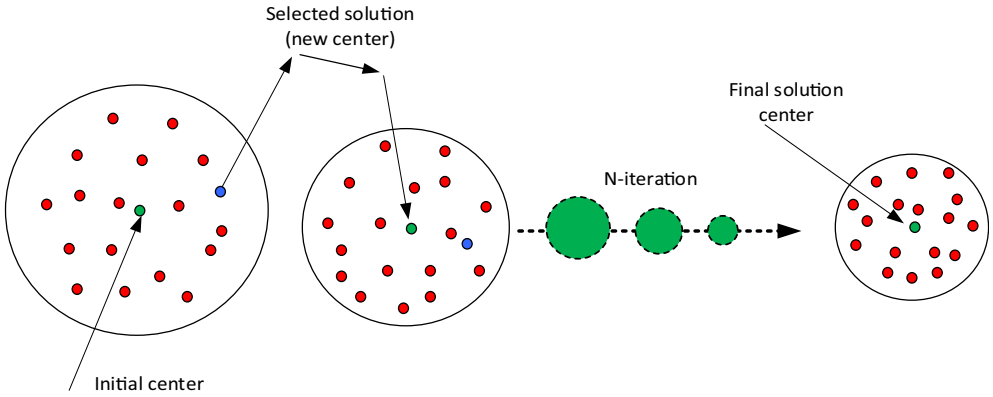

Fig. 2. Representation of the working search process through a model of the VSO in a two-dimensional nested circle form.

search process. In this manner, once the algorithmic rule is terminated, the ensuing pattern develops a vortex-like structure, where the middle of the smallest circle is the optimum solution. In addition, an interpreter pattern is shown in Fig. 3 for a two-dimensional problem exhibiting upper and lower limits between the [−10, 10] interval.

3.2.4. The radius step-down process

The radius step-down process is considered a type of reconciliation step-size adjustment method that is additionally utilized in random search algorithms, and the tactic by which this adjustment is performed is of particular importance for the success of the VSO algorithm. This method should be performed to ensure that it permits the algorithmic program to behave in an exploratory manner in the initial steps and an exploitative manner in the latter steps. To achieve such a process, the value of the radius should be tuned appropriately throughout the search method. A detailed description of the VSO algorithm is presented in the form of a flow chart (see Fig. 4), and further details regarding this process can be found in Ref. [26].

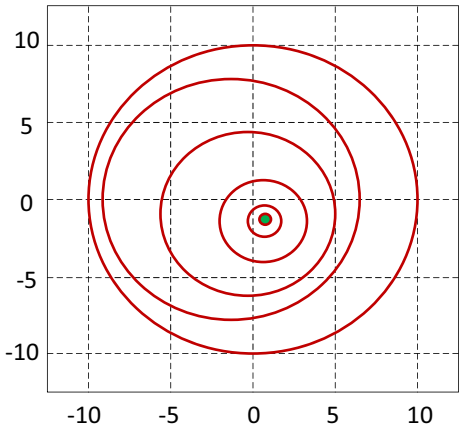

Fig. 3. A vortex-like VSO algorithm representing a search process.

3.3. Constraint handling

To handle the constrained optimization associated with the SMR process, the exterior penalty function (EPF) method was applied to fold the constraints into the objective function [31].

$$\text{Minimize } F(X,p,r_h,r_g) = f(X,p) + P(X,p,r_h,r_g) \tag{8}$$

$$X_i^L \leqslant X_i \leqslant X_i^U \quad i = 1,2,\ldots,\text{n} \tag{9}$$

where r_h and r_g are the penalty constants (multipliers), and $P(X,p,r_h,r_g)$ is the penalty function, which can be expressed as:

$$P(X,p,r_h,r_g) : r_h\left[\sum_{k=1}^{l} h_k(X,p)^2\right] + r_g\left[\sum_{j=1}^{m}(\max\{0,g_j(X,p)\})^2\right] \tag{10}$$

Because the present study was free from the equality constraint, only the inequality constraints were considered.

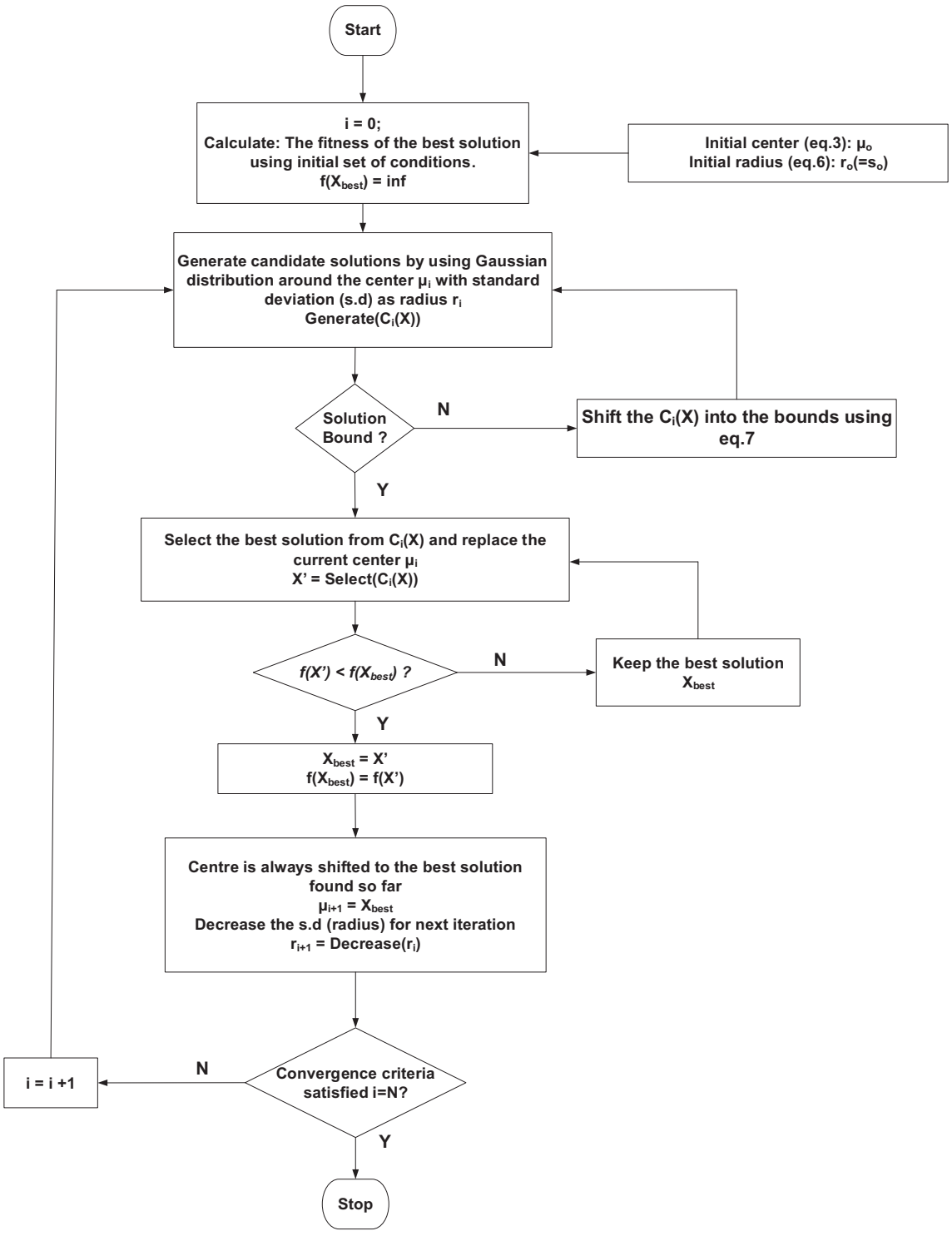

Fig. 4. A working flowchart for the VSO algorithm.

4. Process analysis and optimization results

Through the application of the VSO algorithm, process design optimization was performed by changing the variables within the bounds. When the VSO is employed in the simulation-optimization framework, a trade-off between computational cost (iteration time) and the degree of accuracy exists for the final optimal solution. In this case, an overall compression power saving of $\leq$41.5% was made, and the coefficient of performance (COP) was improved by $\leq$32.8% in comparison with the base case [25]. The design improvement results will now be physically ascertained and understood through composite curve analysis.

Fig. 5a and b [25] shows the temperature difference plot between the composite curves (TDCC) and the temperature-heat flow plot between the composite curves (THCC) inside the cryogenic heat exchanger for the base SMR process, respectively. As indicated, a specific compression power of 0.4584 kW/kg-LNG is required for the base case operational and design parameters.

The TDCC plot shown in Fig. 5 analyzes the effect of the individual refrigerant components on the performance of the liquefaction process, while the composite curves determine the efficiency of the SMR process. These composite curves for the base case indicate that between −80 and 40 °C, a gap of >3 °C exists, which implies enhanced irreversibility, and will ultimately increase the refrigeration cost. To minimize the irreversibility, the gap between the composite curves must be minimized. Thus, the flow rates of the MR ingredients were optimized to address the infeasibility/irreversibility issue and to reduce the energy required during the liquefaction of natural gas. As indicated in Fig. 5a (below the black circled area), a small space between the TDCC curves and the constraint approach temperature of 3 °C is denoted between −160 and −140 °C. In this region, minimization of the exergy losses is low, and further minimization is essential. As the heat transfer performance can be improved by reducing the gaps between the TDCC regions, optimal flow rates for the low boiling point refrigerants, such as nitrogen and methane, must be employed. In contrast, the region inside the green circled area between −95 and −25 °C can easily be improved by determining the optimal flow rates of methane, ethane, and propane. Similarly, an improvement can be achieved between −25 and 40 °C by optimizing the flow rates of the high boiling components propane and *iso*-pentane. These variations ultimately yield to the optimal operational and design parameters for the LNG cryogenic exchanger.

In this study, the proposed SMR process was optimized using several well-known optimization methods (i.e., GA, KBO, and PSO) for comparison purposes and to determine the optimal conditions. These optimization approaches resulted in apparent improvements in the specific compression powers of 0.3183, 0.2887, and 0.2808 kW/kg-LNG, respectively, which are equivalent to energy savings of 30.6, 37.0, and 38.7%, for the GA, KBO, and PSO methods, respectively, when compared to the base case. Finally, the SMR process was optimized by applying the VSO methodology. The resulting optimized conditions therefore resulted in the greatest improvement compared to existing approaches, with a reduction in the specific compression power of ≤0.2681 kW/kg-LNG being achieved, which is equivalent to an energy saving of 41.5% compared with the base case. Table 3 summarizes and compares the optimization results for the VSO methodology with the base case and with the GA-optimized, KBO-optimized, and PSO-optimized cases.

In addition, Fig. 6a and b shows the TDCC and THCC composite curves inside the cryogenic heat exchanger for the VSO-optimized case, respectively.

Note that a high-temperature approach exists inside the main cryogenic heat exchanger between −10 and 40 °C (Fig. 6a). This high-temperature approach is mainly due to the presence of

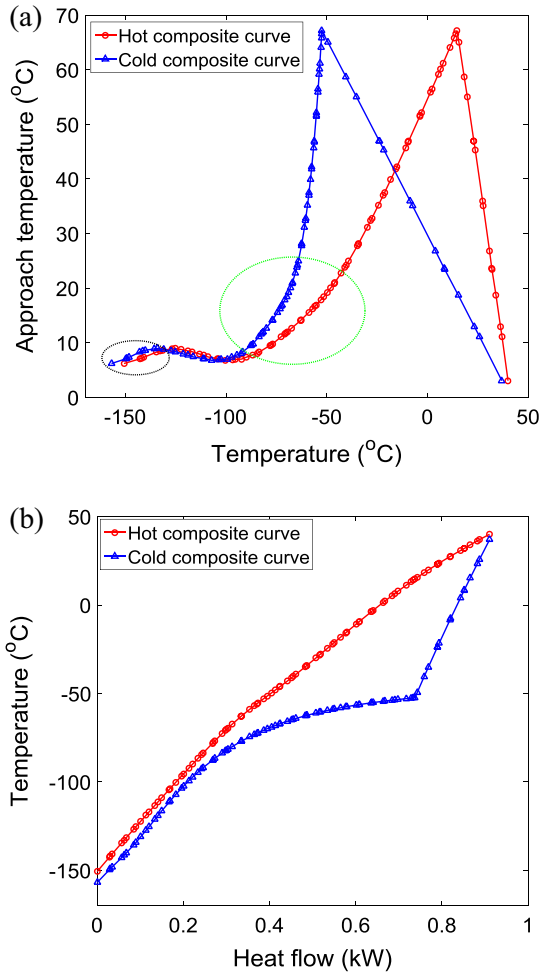

Fig. 5. Composite curves of: (a) TDCC, and (b) THCC for the base case.

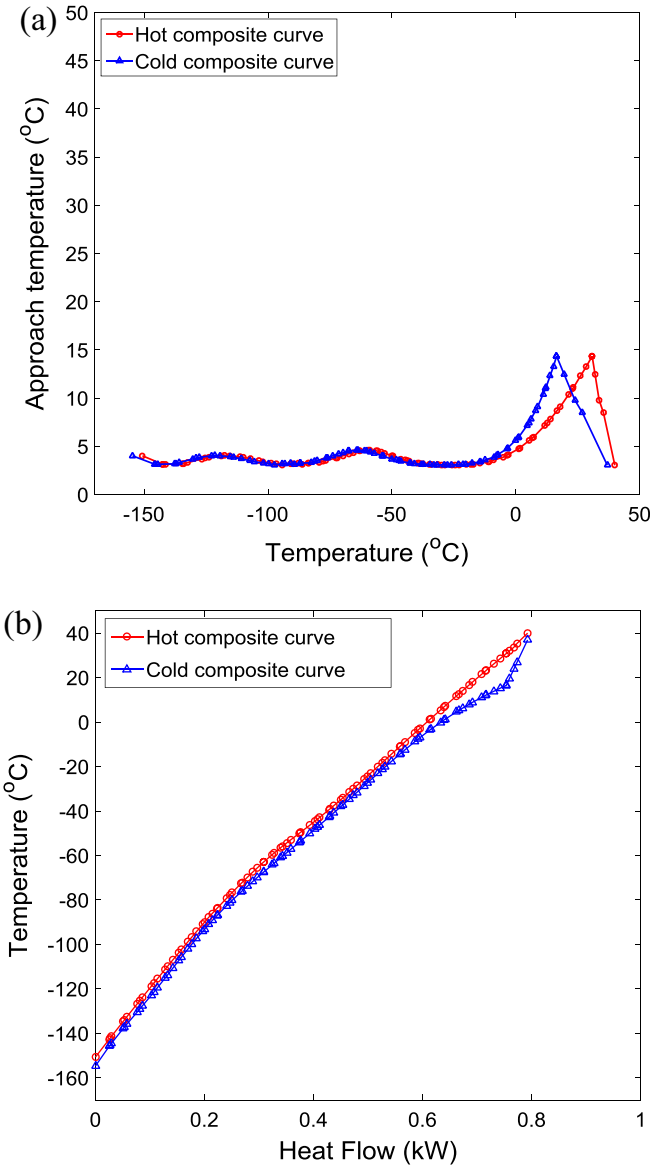

Fig. 6. Optimized (a) TDCC and (b) THCC curves for the VSO-optimized SMR process.

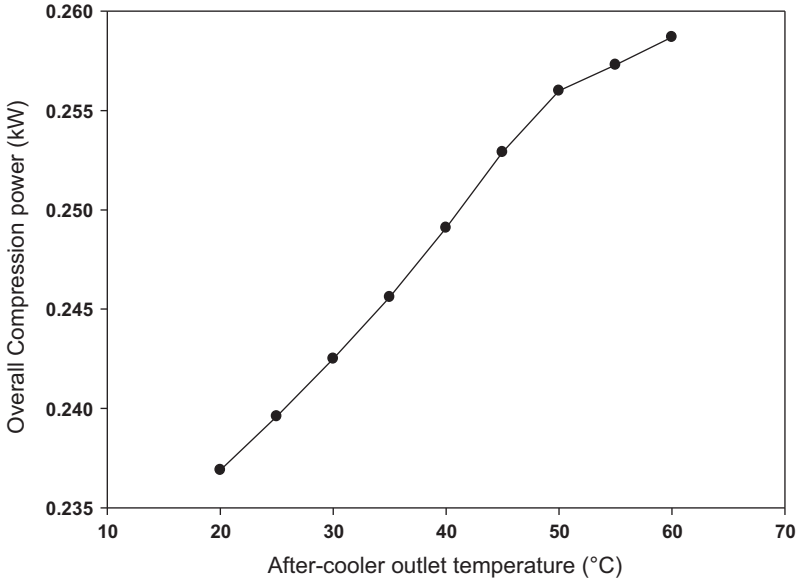

Fig. 7. Influence of the after-cooler outlet temperature on the compression power.

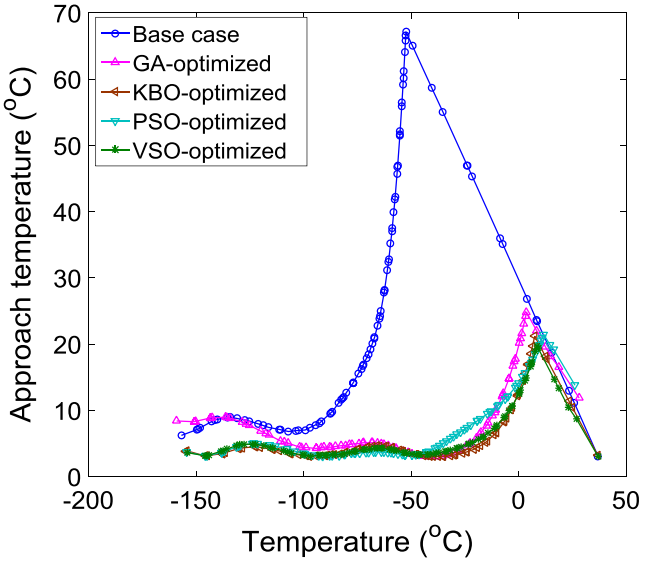

Fig. 8. TDCC comparison between the base case and the optimized cases.

propane and *iso*-pentane and can be further minimized by precooling the natural gas feed and the MR before entry into the main exchanger. Such precooling ultimately enhances the energy efficiency of the process. In addition, it has been reported [9] that the high-temperature approach in the middle section of the composite curves produces irreversibility inside the main cryogenic exchanger, which essentially increases the required specific energy. This high-temperature approach can be shifted to the warmer end of the cryogenic exchanger by increasing the heavy refrigerant flow rate. In the present study, to avoid the formation of a liquid fraction in the K-3 compressor, the heavy refrigerant flow was decreased to maintain the high-temperature approach on the warmer side of the heat exchanger. For the K-2 compressor, the liquid fraction was removed by adjusting the after-cooler temperature. This temperature adjustment resulted in a tradeoff in terms of decreasing the energy efficiency by ~2–3%. Indeed, it can be verified from Fig. 7 that the outlet temperature of the after-coolers produced a proportional impact on the required overall compression power.

Furthermore, the optimal composition of the SMR stream strongly depends on the natural gas feed flow rate and composition with respect to the methane content. The efficiency of the VSO algorithm can be clearly seen in Fig. 8, which compares the composite curves of the VSO-optimized process with those of the base, GA-optimized, KBO-optimized, and PSO-optimized cases. As indicated, the peak of the composite curve for the VSO-optimized SMR process is lower than those of the other optimized curves.

4.1. Design analysis and coefficient of performance

The key role of the LNG cryogenic exchanger relates to the MR capacity for exchanging cold energy with an NG feed to produce the LNG product. Assuming a constant log mean temperature difference (LMTD) and heat transfer area, the performance of the cryogenic exchanger is directly related to the overall heat transfer coefficient, *U*, in the context of energy balance, as indicated in Eq. (11).

$$Q = UA \cdot F_t \cdot (LMTD) \tag{11}$$

As the Aspen Hysys® software does not provide the values of the heat transfer area '*A*' and the heat transfer coefficient '*U*' separately, the required heat transfer area, i.e., a design parameter

Table 4
Design analysis of the SMR process.

Parameters	Base case [25]	KBO Optimized [25]	GA optimized	PSO optimized	VSO optimized
Duty of main cryogenic exchanger (kJ/h)	3277.0	2767.0	2700.0	2808.0	2853.0
Log mean temperature difference (°C)	14.56	4.504	7.52	5.26	4.06
Overall heat transfer coefficient (kJ/C-h)	225.0	614.4	359.3	533.5	702.7
Coefficient of performance (COP)	1.987	2.415	2.59	2.78	2.96

of the exchanger, is examined in terms of the product of the area and heat transfer coefficients (*UA*).

As shown in Table 4, the cooling duty of the main LNG cryogenic exchanger for the VSO-optimized case is less significant than that of the base case (i.e., 2853.0 and 3277.0 kJ/h respectively), but is higher than those of the other optimized cases studies. It should be noted that a greater quantity of cold energy is transferred from the MR to the NG when the LMTD value is higher, as can be seen from the base case of 14.56 °C; however, this higher value also leads to increased entropy generation due to the large temperature gradient.

Furthermore, the LMTD value (4.06 °C) for the VSO-optimized SMR process is lower than the base case, which results in a higher cost for the main cryogenic exchanger at a constant heat transfer coefficient value. This higher investment of the main cryogenic exchanger has an inverse relationship with energy cost in terms of the compression power (see Table 3), with the VSO-optimized case having a significantly higher energy efficiency in comparison with the base case and the other optimized cases. The LMTD can therefore also be considered another important design parameter, which should be optimized to maximize the coefficient of performance (COP) at the most economic and feasible value of *UA*. In addition, the lower heat transfer area value leads to a decrease in capital investment. Furthermore, the LMTD is directly related to the required exchanger area, with an inverse relationship existing between the LMTD value and the exchanger area, as indicated in Eq. (11) above.

The improvement in the exergy efficiency of the process can also be analyzed through the COP of the refrigeration cycle. The COP is defined as the ratio of useful cooling provided to the work input in the form of compression energy, and can be expressed as follows:

$$COP = \frac{Heat\ absorbed\ by\ the\ MR}{Compression\ power} = \frac{Q}{W_{rev}} \tag{12}$$

Furthermore, at the same power source and operating parameters, a higher COP refrigeration cycle usually provides a lower value for the purchased energy compared with that of a lower COP refrigeration cycle. As indicated in Table 4, the refrigeration cycle of the VSO-optimized SMR process yielded the highest COP value among all candidates examined, with a value 32.8% higher than that of the base SMR process being achieved.

5. Conclusions

We herein reported the examination and optimization of the vortex search optimization (VSO) algorithm to enhance the energy efficiency of the single mixed refrigerant-liquefied natural gas (SMR-LNG) process. For this purpose, the augmented Lagrange penalty function was employed to incorporate constraints into the objective function. Thus, the VSO algorithm was successfully employed to determine the optimal values of the key decision variables to ensure a close feasible temperature approach (i.e., 3 °C) between the composite curves over the entire length of the cryogenic LNG exchanger. In addition, the VSO algorithm exhibited superior performance compared to existing optimization algorithms for determining the optimum conditions of the complex SMR process. In particular, using this optimized method, a saving of ≤41.5% could be made on the required compression power compared to the base case. It could therefore be concluded that the VSO algorithm is a simple and efficient method for handling non-linear complex infeasibilities, and so can be applied to other mixed refrigerant-based LNG procedures such as the dual mixed refrigerant, cascade, and propane pre-cooled mixed refrigerant processes.

Acknowledgments

This work was supported by the Basic Science Research Program through the National Research Foundation of Korea (NRF) funded by the Ministry of Education (2015R1D1A3A01015621) and by the Priority Research Centers Program through the National Research Foundation of Korea (NRF) funded by the Ministry of Education (2014R1A6A1031189).

Appendix A. Supplementary material

Supplementary data associated with this article can be found, in the online version, at https://doi.org/10.1016/j.applthermaleng.2017.10.078.

References

[1] SHELL, LNG Outlook 2017, SHELL, 2017.
[2] EIA, Today in Energy, EIA, 2016.
[3] W. Lim, K. Choi, I. Moon, Current status and perspectives of liquefied natural gas (LNG) plant design, Ind. Eng. Chem. Res. 52 (2013) 3065–3088.
[4] A. Finn, G. Johnson, T. Tomlinson, Developments in natural gas liquefaction, Hydrocarbon Process. 78 (1999) 47–56.
[5] M.S. Khan, M. Lee, Design optimization of single mixed refrigerant natural gas liquefaction process using the particle swarm paradigm with nonlinear constraints, Energy 49 (2013) 146–155.
[6] W.-S. Cao, X.-S. Lu, W.-S. Lin, A.-Z. Gu, Parameter comparison of two small-scale natural gas liquefaction processes in skid-mounted packages, Appl. Therm. Eng. 26 (2006) 898–904.
[7] M.S. Khan, I.A. Karimi, D.A. Wood, Retrospective and future perspective of natural gas liquefaction and optimization technologies contributing to efficient LNG supply: a review, J. Natural Gas Sci. Eng. 45 (2017) 165–188.
[8] M. Wang, R. Khalilpour, A. Abbas, Thermodynamic and economic optimization of LNG mixed refrigerant processes, Energy Convers. Manage. 88 (2014) 947–961.
[9] M.S. Khan, S. Lee, G.P. Rangaiah, M. Lee, Knowledge based decision making method for the selection of mixed refrigerant systems for energy efficient LNG processes, Appl. Energy 111 (2013) 1018–1031.
[10] M.A. Ait-Ali, Optimal mixed refrigerant liquefaction of natural gas, 1979.
[11] F.J. Barnés, C.J. King, Synthesis of cascade refrigeration and liquefaction systems, Ind. Eng. Chem. Process Design Dev. 13 (1974) 421–433.
[12] G.C. Lee, R. Smith, X.X. Zhu, Optimal synthesis of mixed-refrigerant systems for low-temperature processes, Ind. Eng. Chem. Res. 41 (2002) 5016–5028.
[13] Y. Shi, A. Gu, R. Wang, G. Zhu, Optimization Analysis of Peakshaving Cycle to Liquefy the Natural Gas-Chapter 174.
[14] M. Mokarizadeh Haghighi Shirazi, D. Mowla, Energy optimization for liquefaction process of natural gas in peak shaving plant, Energy 35 (2010) 2878–2885.
[15] A. Aspelund, T. Gundersen, J. Myklebust, M.P. Nowak, A. Tomasgard, An optimization-simulation model for a simple LNG process, Comput. Chem. Eng. 34 (2010) 1606–1617.
[16] F.D. Nogal, J.-K. Kim, S. Perry, R. Smith, Optimal design of mixed refrigerant cycles, Ind. Eng. Chem. Res. 47 (2008) 8724–8740.
[17] M.S. Khan, S. Lee, M. Lee, Optimization of single mixed refrigerant natural gas liquefaction plant with nonlinear programming, Asia-Pac. J. Chem. Eng. 7 (2012) S62–S70.
[18] A. Morin, P.E. Wahl, M. Mølnvik, Using evolutionary search to optimise the energy consumption for natural gas liquefaction, Chem. Eng. Res. Des. 89 (2011) 2428–2441.
[19] K. Tak, W. Lim, K. Choi, D. Ko, I. Moon, Optimization of mixed-refrigerant system in LNG liquefaction process, Computer-Aid. Chem. Eng. 29 (2011) 1821–1824.
[20] L. Cao, J. Liu, X. Xu, Robustness analysis of the mixed refrigerant composition employed in the single mixed refrigerant (SMR) liquefied natural gas (LNG) process, Appl. Therm. Eng. 93 (2016) 1155–1163.
[21] H. Ding, H. Sun, M. He, Optimisation of expansion liquefaction processes using mixed refrigerant N_2–CH_4, Appl. Therm. Eng. 93 (2016) 1053–1060.
[22] K. Park, W. Won, D. Shin, Effects of varying the ambient temperature on the performance of a single mixed refrigerant liquefaction process, J. Natural Gas Sci. Eng. 34 (2016) 958–968.
[23] M.A. Qyyum, L.Q. Minh, W. Ali, A. Hussain, A. Bahadori, M. Lee, Feasibility study of environmental relative humidity through the thermodynamic effects on the performance of natural gas liquefaction process, Appl. Therm. Eng. 128 (2018) 51–63.
[24] T.N. Pham, M.S. Khan, L.Q. Minh, Y.A. Husmil, A. Bahadori, S. Lee, M. Lee, Optimization of modified single mixed refrigerant process of natural gas liquefaction using multivariate Coggin's algorithm combined with process knowledge, J. Natural Gas Sci. Eng. 33 (2016) 731–741.
[25] T.N. Pham, N.V.D. Long, S. Lee, M. Lee, Enhancement of single mixed refrigerant natural gas liquefaction process through process knowledge inspired optimization and modification, Appl. Therm. Eng. 110 (2017) 1230–1239.

[26] B. Doğan, T. Ölmez, A new metaheuristic for numerical function optimization: Vortex Search algorithm, Inf. Sci. 293 (2015) 125–145.
[27] B. Doğan, T. Ölmez, Vortex search algorithm for the analog active filter component selection problem, AEU – Int. J. Electron. Commun. 69 (2015) 1243–1253.
[28] B. Doğan, A. Yüksel, Analog filter group delay optimization using the Vortex Search algorithm, in: 23nd Signal Processing and Communications Applications Conference (SIU), 2015, pp. 288–291.
[29] M.M.F. Hasan, I.A. Karimi, H.E. Alfadala, H. Grootjans, Operational modeling of multistream heat exchangers with phase changes, AIChE J. 55 (2009) 150–171.
[30] M.S. Khan, I.A. Karimi, M. Lee, Evolution and optimization of the dual mixed refrigerant process of natural gas liquefaction, Appl. Therm. Eng. 96 (2016) 320–329.
[31] P. Venkataraman, Applied Optimization with MATLAB Programming, Wiley, 2009.